

**2011 NDIA GROUND VEHICLE SYSTEMS ENGINEERING AND TECHNOLOGY
SYMPOSIUM
MODELING & SIMULATION, TESTING AND VALIDATION (MSTV) MINI-SYMPOSIUM
AUGUST 9-11 DEARBORN, MICHIGAN**

IMPROVED SAFETY AND MOBILITY OF GROUND ROBOTS

**Huei Peng
A. Galip Ulsoy**
Ground Robotics Reliability Center
University of Michigan
hpeng@umich.edu, 1-734-936-0352

ABSTRACT

The main goal of this paper is to report recent progress on two example projects supported within the Ground Robotics Reliability Center (GRRC), a TARDEC supported research center headquartered at the University of Michigan. In the first project, the concept of Velocity Occupancy Space (VOS), a new navigation algorithm that allows a robot to operate using only a range finding sensor in an unknown environment was developed. This method helps a mobile robot to avoid stationary and moving obstacles while navigating towards a target. The second project highlighted is related to energy and power requirement of mobile robots. Hazardous terrains pose challenges to the operation of mobile robots. To enable their safe and efficient operations, it is necessary to detect the terrain type and to modify operation and control strategies in real-time. A research project supported by GRRC has developed a closed-form wheel-soil model. Computational efficiency of this model is improved by avoiding traditional recursive solution of the model under binary search. Results from these two projects are expected to improve the safety and mobility of mobile robots.

INTRODUCTION

This paper reports recent progress on two selected projects at the Ground Robotics Reliability Center (GRRC), a TARDEC supported research center headquartered at the University of Michigan. The main goal of GRRC is to develop design and analysis tools to promote reliable operations of mobile robots. These two projects are selected from more than a dozen projects currently supported by the Center.

Many of the military mobile robots currently in use were designed to be tele-operated by a soldier. Future mobile robots are likely to become more autonomous. A key enabling technique for autonomous operations is comprehensive environmental awareness, and in particular the existence and motions of nearby obstacles. In addition, the robot needs to plan its motion to avoid colliding with the obstacles while moving toward the target as quickly as possible. Sensing the environment, especially the existence of human objects can be done using different sensing systems. In two recent autonomous robotic competitions: the Grand Challenge and the Urban Challenge, most leading teams selected to use laser range sensors rather than vision cameras as their main "obstacle detection" sensors. In fact, the laser range sensors were used not only to detect obstacles, but also the terrains. The basic idea of the GRRC

safety project is to use information collected from the laser range sensors to avoid collision with moving obstacles. Velocity Occupancy Space (VOS) [1], a new navigation algorithm that allows a robot to operate using only a range finding sensor in an unknown environment was developed. This method can be deployed to avoid stationary and moving obstacles while navigating towards a goal. This method uses the uncertain obstacle representation in the occupancy space to estimate the location of each obstacle and approximate each obstacle's velocity using data in a few steps in the past. The obstacle information is converted into velocity obstacle form and used to calculate the attractiveness of each candidate velocity. The attractive and repulsive factors were weighed and the optimal velocity is picked. Simulation results will be shown to demonstrate the performance of the developed algorithm.

The second project to be highlighted is related to energy and power requirement of mobile robots. Hazardous terrains pose a challenge to the operation of mobile robots, especially for military applications such as surveillance, battlefield casualty extraction, etc. To enable their safe and efficient operations, it is necessary to detect the terrain type and to modify operation and control strategies in real-time. A possible application of the developed concept is for robots used in search and rescue missions, e.g., the concept

UNCLASSIFIED: Dist A. Approved for public release. Disclaimer: Reference herein to any specific commercial company, product, process, or service by trade name, trademark, manufacturer, or otherwise, does not necessarily constitute or imply its endorsement, recommendation, or favoring by the United States Government or the Department of the Army (DoA). The opinions of the authors expressed herein do not necessarily state or reflect those of the United States Government or the DoA, and shall not be used for advertising or product endorsement purposes.

proposed in [2]. These robots may need to traverse through a wide range of terrains and might even switch from tracked to wheeled operations for optimal mobility and energy efficiency. Fast wheel-terrain interaction models suitable for real-time applications are thus important. In a research project supported by GRRC, a closed-form wheel-soil model was developed [3]. Computation efficiency of this model is improved by avoiding traditional recursive solution of the model under binary search. Online prediction and real-time control becomes possible by using the developed closed-form wheel-soil interaction model and the entry angle estimator.

VOS BASED OBSTACLE AVOIDANCE

Several stationary obstacle avoidance algorithms have been developed and successfully implemented, including those described in [4][5]. Path adaption algorithms, such as path-velocity decomposition [6] or gradient-based path planning [7] are often integrated into global planners to allow for reactive behaviors.

The method we developed, based on the *velocity occupancy space* (VOS) concept [1], falls in between the high level global planner and the lower-level obstacle avoidance system. The VOS method uses the *certainty grid* concept to avoid stationary obstacles using uncertain sensor data, as introduced by Moravec and Elfes [8], together with the *velocity obstacle* method for moving obstacle avoidance developed in [9]. Certainty grids allow a robot to navigate in a stationary, cluttered environment using data from a realistically uncertain range sensor (i.e. laser range finder, sonar). The certainty grid deals with the high error rate often found with lower cost range sensors by utilizing multiple sensor measurements.

Conversely, the velocity obstacle concept developed by Fiorini and Shiller [9] and extended by Shiller, Large and Sekhavat [10] and Large, Laugier and Shiller [11] avoids collisions with moving obstacles using a first-order method of motion planning. This method uses information about the obstacles' locations and velocities to compute "velocity obstacles," which are a set of robot velocities that will lead to collision at some future point in time. However, while the velocity obstacle concept allows for the avoidance of moving obstacles, in its original form it requires complete knowledge of the obstacles' dimensions, locations and velocities--information that is typically not available from range finding sensors.

The concept of combining the occupancy grid representation of an uncertain environment with velocity obstacles was first explored by Bis, Peng and Ulsoy [12] and Fulgenzi et al. [13][14]. Fulgenzi et al. use Bayesian Occupancy Filter (BOF) and Probabilistic Velocity Obstacles (PVOs) for velocity selection.

Formulation of Optimization Problem

Assuming that the laser range finders have successfully identified the obstacles in the neighborhood, and calculated their velocities, then each point in the velocity space can be evaluated based on their potential to lead toward a collision and toward the target point. The selection of the robot velocity is solved from an optimization problem, as explained below. The value of each element in the velocity occupancy space is based on two sets of factors. The first set forms a repulsive weight, based on the possibility that this velocity might lead the robot to a collision. The second set is based on how quickly and directly a velocity leads the robot to its goal.

The repulsive value, R , of each element is defined by the equation

$$R = W_R \left[D_R \cdot A_R(W_{AR}) \cdot \left(\frac{W_{TTC}}{TTC} + \frac{1}{CD} \right) \cdot E_{Oc} \right] \quad (1)$$

where the weights (W_R , W_{TTC} , and W_{AR}) are the "degrees of freedom" of the algorithm that can be calibrated or optimized. W_R is the overall repulsive weight; a measure of how important it is to avoid obstacles in comparison to reaching the target. D_R is the repulsive direction term. A_R is the repulsive angular term. The weighted angular term, W_{AR} , allows a more or less conservative range of velocity angles that are assumed to lead to a collision to be defined based on the situation. The time to collision, TTC , and the Cartesian distance, CD , terms characterize the collision risk between the robot and an obstacle. If a velocity does not meet the angle and direction requirements, then the TTC and CD are not calculated, as the overall repulsive weight, R , is already set to zero. E_{Oc} is the occupancy value for the obstacle element with which each robot velocity will lead to a collision.

The attractive value for each VOS element is found from

$$A = [W_{VD} \cdot VD + VC + W_A \cdot A_A] \quad (2)$$

where the weights W_{VD} and W_A are tuned based on the robot's objectives. VD is the difference between the candidate velocity and the desired velocity that will lead toward the goal. VC is the velocity change from the current velocity, used to penalize jerky motions. A_A is the attractive angle computed based on the target location. Details of these terms can be found in [1].

The weights on the repulsive and attractive terms in Eqs.(1) and (2) are first tuned manually and then optimized numerically. The basic process is as follows: 10 representative collision avoidance cases were defined, in which there are one to four moving obstacles, all of them moving at a constant speed (and never pursue the robot maliciously). These obstacles may have speeds that come in

the way between the robot and the target or even directly toward the robot. Therefore, the robot might need to slow down or turn to avoid colliding with these obstacles. These ten cases were used as training scenarios, based on which the weights of the attractive and repulsive terms are optimized.

Four evaluation metrics were used to judge the quality of the path that the robot followed given each set of weights. During each time step the position of the robot, the robot's velocity and the relative position of each obstacle to the robot was recorded. The distance traveled, change in velocity and the square of the inverse of the closest obstacle's proximity to the robot were individually summed for every time step and used as the first three evaluation metrics: distance traveled, acceleration and obstacle proximity. In addition, the number of time steps required for the robot to reach the goal and two binary values that indicated if a collision occurred during the scenario and whether the robot successfully reached the goal were also recorded. Optimization was performed using MATLAB's *fgoalattain()* function to optimize the performance of the algorithm over the ten training maneuvers. This function uses sequential quadratic programming to reduce a set of nonlinear functions to below a given goal level.

Optimization Results

The hand tuned weights and the optimized weights are compared in Table 1.

Table 1 Weights of the VOS algorithm both hand-tuned and optimized

		Hand-tuned Weights	Optimized Weights
Repulsive Weights	W_R	1.0	0.4
	W_{TTC}	3.5	3.5
	W_{AR}	1.0	1.0
Attractive Weights	W_{VD}	2.7	2.2
	W_A	0.3	1.2

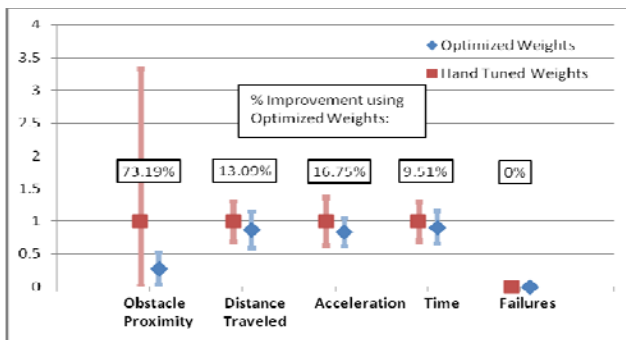


Figure 1: Normalized Evaluation Metrics: Hand Tuned vs. Optimized Weights for 10 Design Scenarios (one sigma error bars)

Performance of the algorithm for the ten training scenarios is shown in Figure 1. The optimized weights result in improved performance in every measure. This result is encouraging but not adequate: since the algorithm was trained using these ten cases it is not a surprise that it performs better for these ten cases.

The performance of the algorithm is then evaluated using one thousand randomly generated scenarios. Due to the randomness, some of the scenarios might be trivial while some others are impossible to handle. Nevertheless, these 1,000 cases cover a wide range of scenarios and represent a comprehensive evaluation of the performance. The optimized algorithm still outperforms the hand-tuned weights consistently, as shown in Figure 2. There were nine failures (0.9%) for the hand-tuned weights and four failures (0.4%) for the optimized weights. The scenarios in which failures did occur were quite challenging. For example, one of the failures using the optimized weights occurred when a couple of obstacles converged almost immediately on the robot. An omniscient agent would have been able to find a successful path; however the algorithm had little time to collect information regarding the obstacles and there were a very limited number of velocity choices that would have allowed the robot to successfully avoid all of the obstacles.

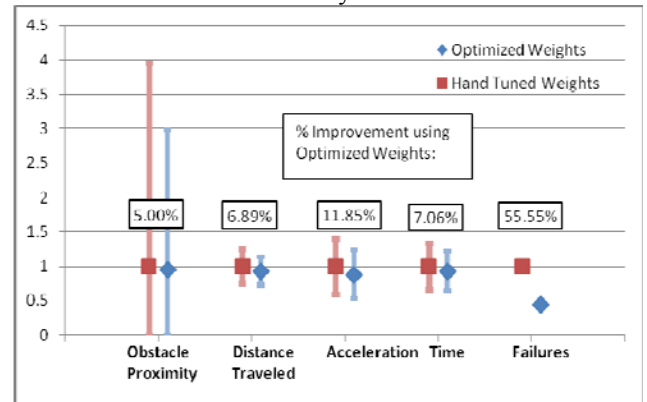


Figure 2: Comparison of Normalized Evaluation Metrics between Hand Tuned and Optimized Weights for 1000 Scenarios (one sigma error bars)

Even though the proposed algorithm assumes that the obstacles move at constant speed, we have also tested its performance with obstacles that have varying speeds. One example is shown in Figure 3. It can be seen that the robot finds a way through these obstacles and reaches the goal successfully.

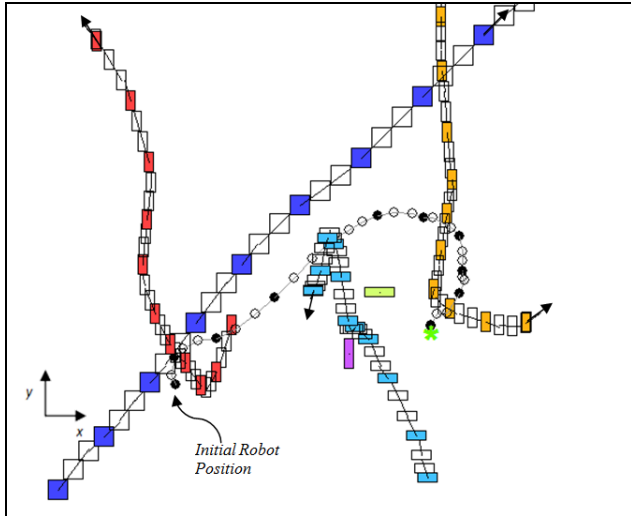


Figure 3: Simulation results with four moving and two stationary obstacles—some with varying speeds

The VOS-based algorithm has demonstrated potential to handle multiple moving obstacles. Currently we are extending the concept presented above to cover the cases when a subset of the obstacles is of higher priority than others (e.g., human pedestrians vs. lifeless objects). It is also possible to use a different sensing system (e.g., far-Infrared) for faster human subject detection. Currently we are implementing the developed algorithm on a mobile robot.

WHEEL-TERRAIN MODEL FOR OFFROAD MOBILE ROBOTS

Military applications often require the robots to travel on unstructured, rugged terrain to conduct tasks such as surveillance or transporting materials. The mobility and trafficability of the robots in these off-road environments are crucial to the success of the mission, with a common failure mode being the robot trapped in soft soil. Another key factor is power consumption, which has become particularly relevant for robots with limited energy source. To achieve a successful mission and improve the mobility and power performance, efficient modeling of locomotion load is required. While existing military robots are mostly track-based, we believe this is because of tradition, rather than the necessary choice. Traditional military vehicles (e.g., tanks and armored vehicles) are very heavy and tracks are clearly beneficial. However, when we are designing for mobile robots around 20-200 pounds, tracked designs can be less efficient than their wheeled counterpart. The fact that NASA Mars Exploration Rover was designed to use six wheels shows that wheeled robots are viable for small robots. In the first phase of our project we focused on the study of wheel-terrain interactions. The track-terrain model is currently under development.

In the mid-20th-century, Bekker studied the principles of off-road vehicle-terrain interactions [15][16] and laid the foundation of terramechanics. The field was later extended by Wong [17][18]. In [19], Wong proposed an analytical model to predict the performance of a driven rigid wheel on soft soil in a straight-line. Inspired by Wong's work, Tran proposed a two-dimensional dynamic model for a skid-steering wheeled UGV on a flat surface [20][21].

The performance of lugged wheel (wheel with grousers) was rarely studied in the literature despite of the fact most wheels designed for off-road applications have grousers. One exception is the wheel-soil model proposed in [22][23]. Unlike Wong's wheel model, where the normal and shear forces are distributed along a cylindrical surface determined by the wheel radius, the normal pressure and the shear stress in this model are assumed to be along surfaces with radii equal to the wheel radius and the shear radius.

The model we developed, called the 'wheel terrain interaction model' (WTIM), incorporates many key concepts from previous studies of terramechanics, including the effect of steering and grousers. Our model was developed for the purpose of both dynamic simulations of mobile robots and for the design and control synthesis of the energy/power system. A common problem of the wheel-terrain interaction models mentioned above is that closed-form expressions of the integrated stress formulas were not available, due to the complexity of classical terramechanics equations. This makes these models time-consuming to solve. On the other hand, online prediction of robot performance is desired to adapt to variable mission conditions, to maximize wheel traction, and/or minimize power consumption. A fast wheel-terrain interaction model is an important enabler toward such online applications.

An accurate, closed-form wheel-terrain interaction model capable of real-time implementation was developed in this GRRC supported project by using quadratic approximation of stress distributions along the wheel-soil interface. The average effect of wheel profiles, e.g., lugs and grousers, will be modeled, with inspiration from classical terramechanics. In addition, the explicit-form solution of the bulldozing resistance contributed by the wheel's side surface in steering maneuvers was developed, based on the stress distribution equations proposed by Bekker [15] and Hegedus [24].

An equally important part of the locomotion model is to integrate the wheel-soil interaction model with a vehicle dynamics model, to calculate motion of the vehicle's body according to wheel contact forces. This is usually done by a multi-body system (MBS) based approach, in which the robot is modeled as an articulated multi-rigid-body system while the wheel contact forces (including the normal forces and tangential forces) are simultaneously identified by the wheel-soil interaction model. This MBS-based approach is flexible and straight-forward. However, it could lead to

numerical stability problems because the normal pressure and wheel sinkage relation is essentially modeled as a non-linear spring. The stability problems remain even after a damping term is introduced. Reduction of oscillations usually requires further tuning of the spring and damping coefficients.

Model Architecture

Figure 4 shows the integrated wheel-soil and vehicle dynamics model. Instead of simultaneously determining the normal and tangential wheel forces, the normal force of each wheel is identified by geometrical analysis and/or classical vehicle dynamics equations. The normal force is then used to determine the longitudinal force, lateral force and moments acting on the wheel. To calculate these forces/torques, we need to determine the entry angle based on the normal wheel load. This is usually solved by iterative methods such as interpolation or recursive binary search, both can be very time-consuming. A non-iterative method to estimate the entry angle is presented in this paper. Online prediction of robot performance and real-time vehicle control become possible by coupling the proposed wheel-soil interaction model and the entry angle estimator. It should be pointed out that this approach could also take advantage of MBS software such as *SimMechanics* and *ADAMS* for vehicle dynamics modeling and system integration.

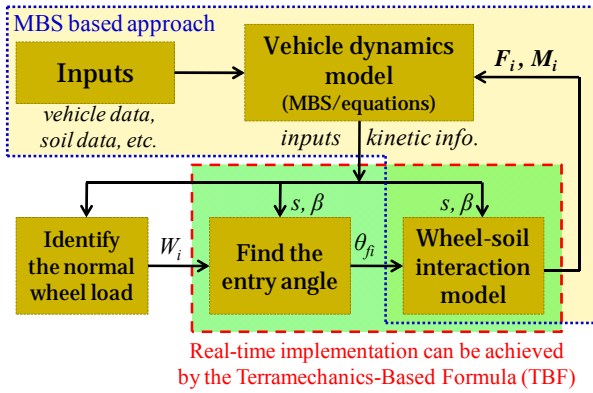


Figure 4. Integrate wheel-soil interaction and vehicle dynamics model.

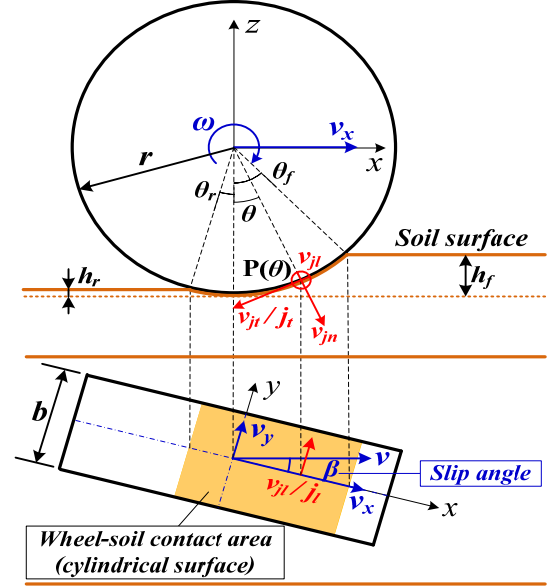


Figure 5. Wheel-soil contact geometry (cylindrical surface).

Figure 5 shows a driven rigid wheel traveling over a flat soil surface. The slip ratio and slip angle of the tires are calculated first, which are then used to calculate the overall shear deformation, the latter is then used to compute the shear stress. Together with the normal stress, the tire forces and moments can then be calculated.

$$\begin{cases} F_x = r_s b \int_{\theta_r}^{\theta_f} (-\sigma_e(\theta) \sin \theta + \tau_{el}(\theta) \cos \theta) d\theta \\ F_y = -r_s b \int_{\theta_r}^{\theta_f} \tau_{el}(\theta) d\theta \\ F_z = r_s b \int_{\theta_r}^{\theta_f} (\sigma_e(\theta) \cos \theta + \tau_{el}(\theta) \sin \theta) d\theta \end{cases} \quad (3)$$

$$\begin{cases} M_x = -r_s^2 b \int_{\theta_r}^{\theta_f} \tau_{el}(\theta) \cos \theta d\theta \\ M_y = -r_s^2 b \int_{\theta_r}^{\theta_f} \tau_{el}(\theta) d\theta \\ M_z = -r_s^2 b \int_{\theta_r}^{\theta_f} \tau_{el}(\theta) \sin \theta d\theta \end{cases} \quad (4)$$

Notice that Eqs. (3) and (4) can be solved analytically if the stress distribution equations are polynomials of θ . In fact, a linear approximation method was used to develop a closed-form wheel-terrain interaction model for straight-line motion scenarios [25]. However, the stresses are generally nonlinear, and the linear approximation sometimes leads to large errors. This is especially true if the soil's sinkage exponent n is small (e.g., clayey soil). We use a quadratic approximation method in this paper because the model accuracy is improved significantly with minimal increase in computational load.

Simulations were conducted to compare the performance of the quadratic approximation with respect to the original nonlinear model (solved iteratively) over a broad parameter space. Three typical soils with different sinkage exponents are chosen and their physical properties are given in Table 2 [25]. Both the smooth wheel and the lugged wheel are studied and their geometry parameters are given in Table 3. The other parameters required for the simulations are given in Table 4.

Table 2. Physical parameters of the selected soils.

Parameter (unit)	Description	Dry sand	Sandy loam	Clayey soil
n (-)	Sinkage exponent	1.1	0.7	0.5
c (kPa)	Cohesion	1.0	1.7	4.14
ϕ (°)	Internal friction angle	30	29	13
k_c (kN/m ⁿ⁺¹)	Cohesive modulus	0.9	5.3	13.2
k_ϕ (kN/m ⁿ⁺²)	Frictional modulus	1523	1515	692.2
K (m)	Shear modulus	0.025	0.025	0.01

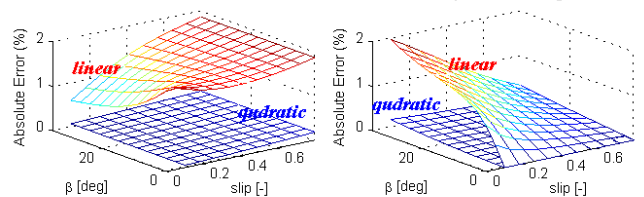
Table 3. Parameters of the smooth wheel S and lugged wheel L.

Parameter (unit)	b (m)	r (m)	l_g (m)	r_s (m)	μ (-)
Smooth wheel S	0.075	0.080	0.0	0.080	0.0
Lugged wheel L	0.075	0.080	0.005	0.085	0.1

Table 4. Other parameters used for model comparison.

Parameter (unit)	s (-)	β (°)	θ_f (°)	θ_m (°)	θ_r (°)
Value	[0.1, 0.8]	[0, 36]	[20, 50]	$\theta_f/2$	0

Error(Tx=F_x/F_z): $e_1=1.51\pm0.30\%$; $e_2=0.11\pm0.04\%$ Error(Ty=F_y/F_z): $e_1=0.60\pm0.51\%$; $e_2=0.04\pm0.03\%$



Error(F_z): $e_1=20.37\pm0.29\%$; $e_2=1.96\pm0.05\%$ Error(My): $e_1=13.19\pm2.39\%$; $e_2=1.35\pm0.13\%$

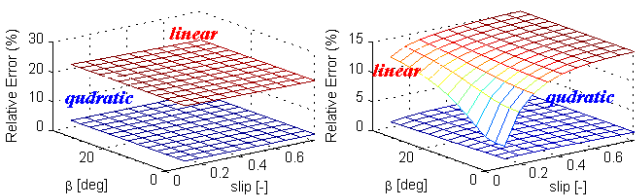


Figure 6. Approximation errors at various slip conditions (smooth wheel on sandy loam).

Figure 6 shows the errors of the linear and quadratic approximation methods against the original nonlinear model for various slip ratios and slip angles under the same entry angle θ_f ($\theta_f = 30^\circ$). The mean values and the standard deviations of these errors can then be plotted relative to the entry angle for the smooth wheel and lugged wheel over these soils, as shown in Figure 7. The mean values of the approximation errors are given in the subplots. The notations 'S1' and 'S2' represent the linear and quadratic approximations of the stresses for the smooth wheel S, respectively. The notations 'L1' and 'L2' represent those of the lugged wheel L. We see that the modeling error is reduced by an order of magnitude by using the quadratic approximation method.

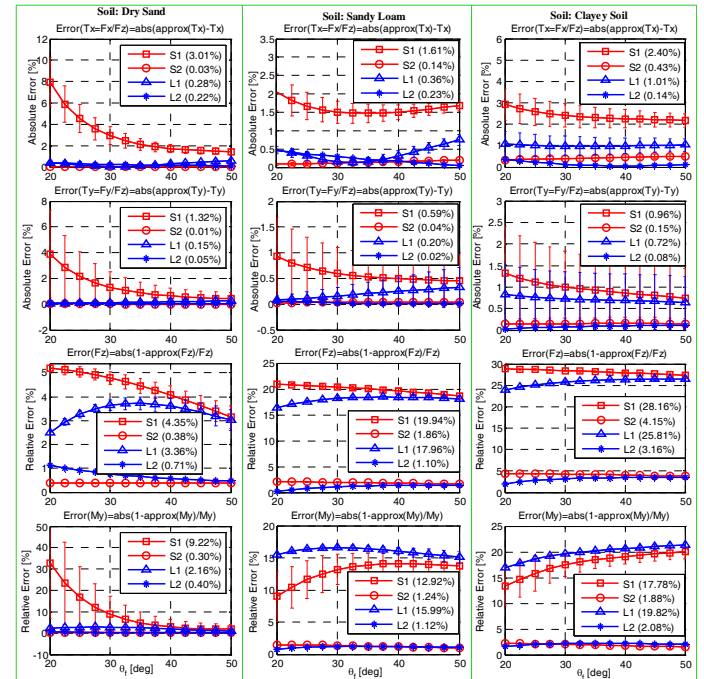


Figure 7. Error statistics of the quadratic and linear approximation methods.

The wheel-soil interaction model was compiled as C-MEX files to interface with Matlab/Simulink. Overall computation times of these three functions are 277 μ s on a 1.6 GHz laptop computer. This demonstrates the feasibility for online applications.

Simulation and Experimental Validations

The simulation procedure is summarized as follows:

1. Initialize the vehicle dynamics model and the wheel-terrain interaction model. Set the robot's initial acceleration to zero.
2. Determine the normal load of each wheel.

3. Update the steering angles and the rotational angular velocities for each wheel according to the data measured in experiments. Calculate the slip ratios and slip angles.
4. Derive other forces/torques for each wheel by using TBF.
5. Obtain the robot's positions, orientation (yaw angle), and velocities. Return to step 2.

Instead of using the above procedure, one can also use MBS software such as *Open Dynamics Engine (ODE)* or *ADAMS* for vehicle dynamic modeling and system integration. The *SimMechanics* Toolbox in *Matlab/Simulink* is used in this paper. As shown in Figure 8, the robot (the steering angle of each wheel is fixed in this example) is modeled as a rigid body with three degrees of freedom (DOFs). The wheel-soil interaction for each wheel is handled by a TBF block.

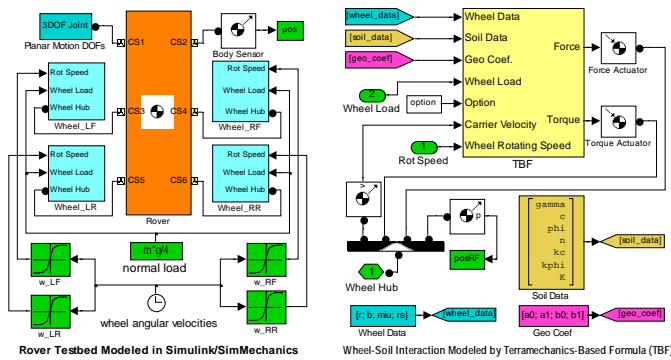


Figure 8. Rover testbed modeled in Simulink with wheel-soil interactions handled by TBF.

In addition to simulations, we also conducted experiments on a 4-wheel rover designed and assembled at GRRC (see Figure 9). Figure 10 shows the comparison between the simulation and experimental results of two steering experiments. The simulation results are very close to the experimental results, with the mean error approximately at 3.5% of the true (experimental) values. This is a significant reduction from a “convention model” which is the standard “bicycle model” commonly used in the automotive field.

In addition to the standard on-board sensors, a state-of-the-art motion capture system (Vicon MX series, accuracy: sub-mm) was used to record the robot's trajectory at a rate of 60 Hz. Thirteen reflective markers (5 markers on the rover body, 2 markers on each of the suspension arms, and 1 marker on each of the steering blocks) were installed on the rover testbed for motion tracking. When the high accuracy tracking system is used, the RMS position error and the final state position error are 1.18 cm and 0.44 cm, respectively

when the robot travels 1m. Those of the orientation error are 0.27 deg and 0.23 deg, respectively. The proposed model also exhibits good accuracy in predicting translational speeds of the vehicle center and the rover's wheels.

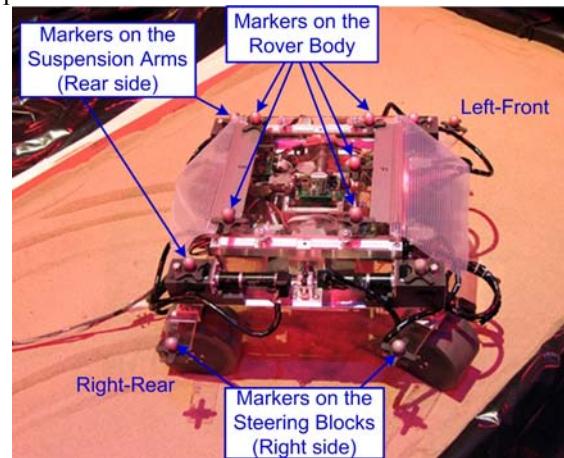


Figure 9. The test robot with motion tracking system.

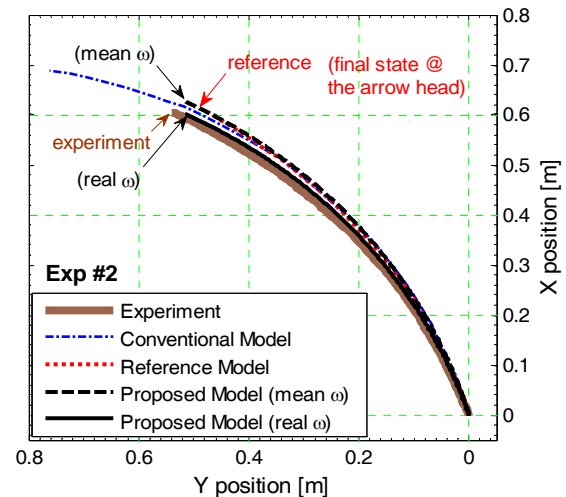
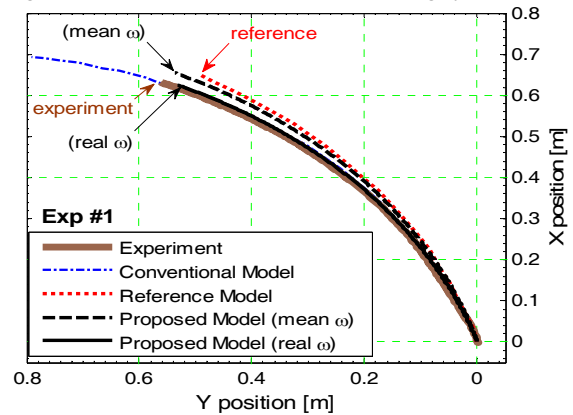


Figure 10. Experimental and simulation results of rover steering trajectories.

CONCLUSIONS

The Ground Robotics Reliability Center focuses on innovative research to improve the reliability of mobile robots. The two example projects presented in this paper aim to achieve reliable operations through improved environmental awareness, and improved efficiency. The final goal is better safety and mobility of ground robots. The VOS based navigation algorithm achieves excellent obstacle avoidance performance. Its performance has been validated using 1,000 randomly created scenarios. This algorithm is now being implemented on a super-droid mobile robot.

The terramechanics model developed combines key elements presented in the literature, including the effect of steering and grouser. We are working on off-line processes to improve the computation efficiency, as well as applying it to the sizing of power component of a conceptual robot.

Acknowledgement

This research was supported in part by the Ground Robotics Reliability Center (GRRRC) at the University of Michigan, with funding from government contract DoD-DoA W56H2V-04-2-0001 through the Ground Vehicle Robotics group at TARDEC (Unclassified. Dist. A. Approved for public release).

REFERENCES

- [1] R. Bis, H. Peng, and A.G. Ulsoy, "Velocity Occupancy Space: Autonomous Navigation in an Uncertain, Dynamic Environment", Accepted for publication in *International Journal of Vehicle Autonomous Systems*, 2011.
- [2] <http://www.vecna.com/robotics/multimedia/downloads/BEAR.pdf>.
- [3] Z. Jia, W. Smith and H. Peng, "Terramechanics based wheel-terrain interaction model (WTIM) and its applications to off-road wheeled mobile robots", Accepted for publication in *Robotica*, 2011.
- [4] J.C. Latombe, *Robot Motion Planning*, Kluwer: Boston, 1991.
- [5] S. Thrun, W. Burgard, and D. Fox, *Probabilistic Robotics*, The MIT Press, Cambridge, 2005.
- [6] K. Kant, and S. Zucker, "Toward efficient trajectory planning: The path-velocity decomposition", *International Journal of Robotics Research*, Vol. 5, No.3, pp. 72-89, 1986.
- [7] K. Konolige, "A gradient method for real time robot control". *Proceedings of the IEEE/RSJ International Conference on Intelligent Robots and Systems*, pp. 639-646, 2000.
- [8] H. Moravec, and A. Elfes, "High resolution maps from wide angle sonar". *Proceedings of the 1985 IEEE International Conference on Robotics and Automation*, pp. 116-121, 1985.
- [9] P. Fiorini, and Z. Shiller, "Motion planning in dynamic environments using velocity obstacles", *International Journal of Robotics Research*, Vol. 17, No. 7, pp. 760-772, 1998.
- [10] Z. Shiller, F. Large and S. Sekhavat, "Motion planning in dynamic environments: Obstacles moving along arbitrary trajectories". *Proceedings of 2001 IEEE International Conference on Robotics and Automation*, pp. 3716-3721, 2001.
- [11] F. Large, C. Laugier, and Z. Shiller, "Navigation among moving obstacles using the NLVO: Principles and applications to intelligent vehicles", *Autonomous Robots*, Vol.19. No. 2, pp. 159-171, 2005.
- [12] R. Bis, H. Peng, and A.G. Ulsoy, "Velocity Occupancy Space: Robot Navigation and Moving Obstacle Avoidance with Sensor Uncertainty". *Proceedings of the 2009 Dynamic Systems and Controls Conference*. October, 2009.
- [13] C. Fulgenzi, A. Spalanzani, and C. Laugier, "Dynamic Obstacle Avoidance in uncertain environment combining PVOs and Occupancy Grid". *Proceedings of the 2007 IEEE International Conference on Robotics and Automation*, pp. 1610-1616, 2007.
- [14] C. Fulgenzi, "Autonomous navigation in dynamic uncertain environment using probabilistic models of perception and collision risk prediction", PhD thesis. Institut National Polytechnique de Grenoble.
- [15] M. G. Bekker, *Theory of Land Locomotion*. The University of Michigan Press, Ann Arbor, 1956.
- [16] M. G. Bekker, *Introduction to Terrain-Vehicle Systems*. The University of Michigan Press, Ann Arbor, 1969.
- [17] J. Y. Wong, *Terramechanics and Off-road Vehicles*. Elsevier, Amsterdam, 1989.
- [18] J. Y. Wong. *Theory of Ground Vehicles* (4th edition). John Wiley & Sons, Aug. 2008.
- [19] J. Y. Wong and A. R. Reece, "Prediction of rigid wheels performance based on analysis of soil-wheel stresses, part I. performance of driven rigid wheels", *J. Terramechanics*, 4(1), 81-98, 1967.
- [20] T. H. Tran, N. M. Kwok, S. Scheduling and Q. P. Ha, "Dynamic Modeling of Wheel-Terrain Interaction of a UGV", the 3rd Annual IEEE Conference on Automation Science and Engineering, Scottsdale, AZ, USA, pp. 369-374, 2007.

- [21] T. H. Tran, "Modeling and Control of Unmanned Ground Vehicles", Ph.D. Thesis. Sydney, Australia: the Faculty of Engineering, University of Technology, Sydney, 2007.
- [22] L. Ding, H. Gao, Z. Deng, K. Yoshida and K. Nagatani, "Slip ratio for lugged wheel of planetary rover in deformable soil: definition and estimation", IEEE International Conference on Intelligent Robots and Systems (IROS 2009), St. Louis, USA pp 3343-3348.
- [23] L. Ding, "Wheel-soil interaction terramechanics for lunar/ planetary exploration rovers: modeling and application", Ph.D. Thesis. Harbin, China: School of Mechatronics Engineering, Harbin Institute of Technology, 2009.
- [24] Hegedus, E., "A simplified method for the determination of bulldozing resistance," Land Locomotion Research Laboratory, Army Tank Automotive Command Report, 61, 1960.
- [25] Shibly, H., Iagnemma, K., & S. Dubowsky, "An Equivalent Soil Mechanics Formulation for Rigid Wheels in Deformable Terrain, with Application to Planetary Exploration Rovers." Journal of Terramechanics, 42(1), 1-13, 2005.